

Joint Centre for Mesoscale Meteorology, Reading, UK



Convective Frontogenesis

A. J. Thorpe
D. J. Parker

Internal Report No. 27

April 1994

Met Office Joint Centre for Mesoscale Meteorology Department of Meteorology
University of Reading PO Box 243 Reading RG6 6BB United Kingdom
Tel: +44 (0)118 931 8425 Fax: +44 (0)118 931 8791
www.metoffice.com



Convective Frontogenesis

DOUGLAS J. PARKER AND ALAN J. THORPE

Department of Meteorology, University of Reading, UK.

ABSTRACT

It is shown here that there exists a regime of balanced frontogenesis which is forced almost entirely by the diabatic heating due to convection at a front. This theory is explored in the context of the horizontal shear frontogenesis exhibited by the two dimensional semigeostrophic equations with an Eady basic state. As convection at fronts is, at low levels, due to the moisture convergence of the cross-frontal ageostrophic flow, the model described here uses a CISK parametrization scheme. The significant result is that the growth rate of the convective frontal system becomes independent of the total wavelength of the domain, once the diabatic heating exceeds a relatively large threshold magnitude. In this regime the frontal zone has a width and structure dependent on the heating magnitude but not on the wavelength. The system is described as 'solitary' or 'isolated' since the dynamics are self-contained and independent of the far-field.

The energetics of the system have a diabatic conversion which is an order of magnitude greater than that due to the large scale along-front temperature gradient. The large scale forcing is, however, necessary as a catalyst, in maintaining a weak ageostrophic convergence which allows the convective heating to be triggered. The constraint of along front geostrophic balance means that convective forcing alone cannot maintain frontogenesis. It is suggested that the convectively dominated front has features of its behaviour which bear a similarity to a mid-latitude squall line. This may be the reason why synoptic fronts can often spawn such squall lines.

The propagation and dynamics of the front are interpreted in terms of the notion of a 'diabatic Rossby wave'.

1. Introduction

The study of atmospheric fronts at which convection occurs has taken two main directions, pursuing the models of 'synoptic front' or 'squall line'. In the study of synoptic fronts it is now thought that mesoscale processes may be significant while synoptic scale influences are considered to exert an influence on squall line behaviour. Here we suggest that a spectrum of convective frontal systems exists which, in general, exhibits features of both basic models. The Bergen school initially referred to the cold front of a midlatitude cyclone as the 'squall line'; more recently, cases have been documented in which systems classed as 'squall lines' have been initiated as a 'synoptic cold front'. Meischner *et al.* (1991) and Cram *et al.* (1992) discuss such observations: in both cases the squall line propagated ahead of its region of genesis. Such a feature raises important questions for forecasting. Since the propagation speeds and propagation mechanisms of the two theoretical models are different, that of a synoptic wave being determined by the large-scale structure of potential vorticity (pv) and temperature gradients and that of a squall line by buoyancy processes at the cold pool, it is important to understand the behaviour of systems for which synoptic forcing and convective processes are both strong. This understanding is the basic aim of this paper.

Synoptic fronts are perceived to be formed as singularities of synoptic scale flows and are seen to form in dry models (e.g. Thorncroft, Hoskins and McIntyre, 1993). Moist processes are seen as modifying the development. For instance, the diabatic heating parametrization of Thorpe and Emanuel, 1985, (ThEm) for synoptic systems acts to reduce the effective static stability of the atmosphere in regions of condensation: in effect this means that flows may be seen in terms of conceptual balanced 'dry' dynamics. However, on smaller scales such a picture may be inaccurate. Observations of fronts involving active convection (such as Browning and Harrold, 1970, or Hobbs and Persson, 1982) tend to exhibit intense, narrow updraughts and there has been speculation (as in

Hobbs and Persson, 1982) that the cold front may act as a gravity current, for which balanced dynamics may be inadequate.

On the mesoscale, squall lines have been seen as representing an organisation of intense convection and have been successfully modelled without the consideration of planetary rotation. However, recent work has suggested that the larger scale flows associated with a squall line may be extremely important in conditioning its environment (Lafore and Moncrieff, 1990; Garner and Thorpe, 1992) and the balanced response to such systems may be crucial to their longevity. Similarly, work of Fovell (1991) has shown how the existence of a balanced baroclinic basic state on a rotating plane may help to maintain a squall line.

Craig and Cho, 1988 (CC88), in studying convective heating in polar lows, were able to exhibit a theoretical regime in which diabatic processes are dominant over baroclinic instability. The modelled waves showed a smooth transition between essentially 'dry' behaviour and moist dominance as the intensity of the diabatic heating was increased. The moist-dominated modes showed a rather different structure to the dry wave, with strong vertical motion and significant potential vorticity anomalies on the boundaries of the convection. Although balanced and not admitting gravity wave behaviour, such a model will be used here to suggest the existence of an intermediate regime linking synoptic fronts and squall lines, in that the balanced model may become dominated by the convective heating. An extreme model of the diabatically dominated regime was provided by Snyder and Lindzen (1991) who constructed growing modes in an infinite baroclinic fluid, in which the heating was bounded by horizontal levels: this flow is not baroclinically unstable and the growth of waves is provided solely by the diabatic processes.

CC88's growing waves were constructed, for analytical simplicity, with symmetry between columns of heating and cooling; an 'unconditional' parametrization. However, the

dynamics of observed systems are rather different, with strong asymmetry between narrow, convectively heated updraughts and broader, more nearly adiabatic downdraughts. A more realistic representation of diabatic processes would involve 'conditional' heating for which only the positive diabatic heat source is included. In the case of the ThEm parametrization, the conditional form produces a marked scale interaction between 'moist' and 'dry' dynamics and the different roles of diabatically induced potential vorticity anomalies and boundary temperature anomalies of a flow. In the ThEm case, however, the pure dry and pure (unconditional) moist modes have equivalent dynamics: in a conditional version of CC88's waves a more complicated dry/moist interaction may be expected as the moist mode is dynamically rather different to the dry. It is the conditional version of CC88's system which is numerically modelled and discussed in this paper. It will be shown that the moist-dominated regime exists within the conditional formulation and, furthermore, that new properties are exhibited. The convective fronts are self-contained or 'solitary' and as such represent a link between the studies of 'squall lines' and 'synoptic fronts'.

2. The Semigeostrophic Equations

The semigeostrophic (SG) equations (Hoskins and Bretherton, 1972) allow the study of frontal features which are almost geostrophic in one horizontal direction but may have strong vertical component of vorticity. They are ideally suited to the study of quasi-two dimensional regions of strong baroclinicity in which the balanced winds may be strong, provided the cross frontal ageostrophic flow is relatively weak. Observations from the FRONTS 87 experiment, analysed by Thorpe and Clough (1991) indicate that this assumption of geostrophy may be a good approximation in frontal regions. Under the geostrophic momentum approximation (Hoskins, 1975) it is significant that, in contrast to the quasigeostrophic (QG) system, the advection of momentum by the ageostrophic wind is not small and is retained. Here the two dimensional form is

assumed and the front will always be taken to lie parallel to the y ('meridional') axis. Summaries are found in Gill (1982, pp 571-578) and ThEm.

The system is simplified by transformation to 'geostrophic coordinates',

$$X = x + \frac{v_g}{f}, \quad Z = z, \quad (1)$$

to give analogous equations to the quasigeostrophic system. In particular, redefining the geostrophic streamfunction by $\Phi = \phi + \frac{1}{2}(v_g^2 + u_g^2)$, the thermal wind equations may be shown to hold in the new system.

Neglecting some nonlinear terms which are thought to be small, the semigeostrophic potential vorticity, q , is defined as,

$$q = \frac{1}{\rho} \zeta \frac{\partial \theta}{\partial Z}, \quad (2)$$

in which ζ is the vertical component of vorticity and the pv tendency follows,

$$\frac{Dq}{DT} = \frac{\zeta}{\rho} \frac{\partial S}{\partial Z}, \quad (3)$$

where $S \equiv \frac{D\theta}{DT}$ and $T \equiv t$ is used to emphasise the change of coordinates. Note that positive heating produces negative anomalies of pv above and positive anomalies of pv below the heating region.

Thermal wind balance gives for the inversion equation,

$$\frac{\partial^2 \Phi}{\partial X^2} + \frac{\theta_0 f^3}{g \rho q} \frac{\partial^2 \Phi}{\partial Z^2} = f^2, \quad (4)$$

which is generally solved subject to boundary conditions of a specified field of $\theta = \frac{\theta_0}{g} \Phi_Z$. Now the semigeostrophic equations are the same for modified geostrophic streamfunction, Φ , as those for ϕ in quasigeostrophy. The coupling with ageostrophic

motion occurs in the $w \frac{\partial}{\partial Z}$ term of the Lagrangian derivative; this is zero for advection on the boundaries. When moist processes are introduced, the heating will depend on vertical velocity and ageostrophic effects will feed back through the pv tendency in (3) and the advection.

Continuity implies that the ageostrophic flows for the two dimensional system may be expressed in terms of a streamfunction, ψ , defined such that,

$$u_{ag} = \frac{1}{\rho} \frac{\partial \psi}{\partial z}, \quad w = -\frac{1}{\rho} \frac{\partial \psi}{\partial x}, \quad (5)$$

which is calculated via the Boussinesq Sawyer-Eliassen (S-E) equation:

$$\frac{\partial^2 \psi}{\partial Z^2} + \frac{\partial}{\partial X} \left(q \frac{g\rho}{f^3 \theta_0} \frac{\partial \psi}{\partial X} \right) = -2Q - \frac{g\rho}{f^2 \theta_0} \frac{\partial S}{\partial X}. \quad (6)$$

This is generally solved subject to the kinematic boundary condition of zero normal flow, or $\psi = 0$, on the boundaries. The geostrophic forcing term, Q , is defined as,

$$Q \equiv -\frac{g\rho}{f^2 \theta_0} \left(\frac{\partial u_g}{\partial X} \frac{\partial \theta}{\partial X} + \frac{\partial v_g}{\partial X} \frac{\partial \theta}{\partial Y} \right), \quad (7)$$

and involves only geostrophic quantities: the S-E equation is purely diagnostic.

The scheme for solving the SG equations consists of inverting pv using (4), with boundary conditions of θ , constructing Q from the geostrophic fields to solve the S-E equation and using the wind fields to advect pv and boundary θ .

The inversion equation (4) and the S-E equation (6) will both be elliptic provided the potential vorticity, q , is strictly positive throughout the domain. In physical terms this means that the flows are stable to symmetric instability (Hoskins, 1974). In the absence of heating, the ellipticity of (6) guarantees the uniqueness of its solutions: this property is essential in the evaluation of semigeostrophic flows. For certain diabatic

heating formulations, such as unconditional CISK, free solutions of the S-E equation (6) can exist, as shown by Parker (1993). In such a case, there is no way of explicitly determining the ageostrophic flow of the system, and the problem cannot be solved without the imposition of other arbitrary conditions. However, for the conditional form of heating used here, free solutions do not appear to exist.

3. Shear Frontogenesis

a. Formulation of the Dynamics

Here we consider frontogenesis forced by horizontal wind shear. A simple framework for such frontogenesis is provided by the Eady wave within which frontal regions form via the shear mechanism. The basic state is a constant balanced shear with height in the zonal direction.

Using the numerical model described in Emanuel, Fantini and Thorpe, 1987 (EFT), waves, incorporating diabatic processes and pv anomalies, will be integrated into the nonlinear regime. In the results described here, a grid of 40 levels in the vertical and 129 steps in the horizontal is employed. The basic state for the waves is a linear geostrophic shear $\overline{\frac{du_g}{dZ}} = 3.0 \times 10^{-3} s^{-1}$ with a corresponding meridional temperature gradient $\overline{\frac{d\theta}{dY}}$ (constant) in thermal wind balance. Other parameter values used are tropopause height, $H = 10 \text{ km}$, Coriolis parameter, $f = 10^{-4} s^{-1}$ and static stability, $\overline{\theta_Z} = 4 \times 10^{-3} K m^{-1}$.

b. A Link Between Ageostrophic and Geostrophic Flow

For the Eady basic state there is a simple rule-of-thumb that will be applied in the subsequent work, in the deduction of vertical velocity from geostrophic motion. Considering the forcing of the cross frontal flow in (6),

$$\begin{aligned} \frac{\partial^2 \psi}{\partial Z^2} - \frac{\partial}{\partial X} \left(q \frac{g\rho^2}{\zeta f^2 \theta_0} w \right) \\ = -\frac{g\rho}{f^2 \theta_0} \frac{\partial}{\partial X} \left(2v_g (-\overline{\theta_Y}) + S \right). \end{aligned} \quad (8)$$

Here the meridional temperature gradient, $\overline{\theta_Y}$, is taken to be negative so that, in effect, positive v_g acts in the same way as S , as positive heating on the r.h.s. of the S-E equation; this is the geostrophic thermal advection. Using simple scaling in (8) an integral of this equation may be estimated as,

$$w \sim \frac{1}{\theta_Z} (2v_g (-\overline{\theta_Y}) + S), \quad (9)$$

provided the horizontal scale of the ageostrophic motion is less than the Rossby radius, as is generally the case for a diabatically heated updraught, in which case the first term of (8) may be neglected. This rule, which is suggested by Snyder and Lindzen's (1991) equation (17), will be used to estimate the ageostrophic flow from the geostrophic fields. Although it can fail in extreme cases, close to physical boundaries or if the first term of (8) is large, generally updraughts are associated with positive v_g (positive thermal advection) and vice versa. Since vertical motion tends to produce vortex stretching in the lower region of the updraught, the low level jet tends to increase the vorticity locally. The relation between these effects gives a wave its particular structure. At this stage it should also be noted that since Q is directly proportional to the basic state meridional temperature gradient, there can be no Q -forcing of ageostrophic flow without the basic baroclinicity, regardless of the geostrophic flow perturbation.

c. *Energetics*

Energy terms are evaluated, as in CC88, in the form,

$$GE = \frac{1}{2} \frac{g}{\theta_0} \frac{1}{\theta_Z} \overline{(\theta' S)}, \quad (10)$$

$$CE = -\frac{1}{2} \frac{g}{\theta_0} \overline{(w \theta')}, \quad (11)$$

$$CA = \frac{1}{2} \frac{f \overline{u_Z}}{\theta_Z} \overline{(v'_g \theta')}. \quad (12)$$

where GE is the conversion from diabatic heat sources to eddy available potential energy, CA is the conversion from basic state to eddy available potential energy and CE is the conversion of eddy available potential energy to eddy kinetic energy. These relations are obtained following a method analogous to that of Gill (1982 p 565) for the quasigeostrophic equations. The ratio $\frac{GE}{CA}$ will be used to illustrate the relative roles of the diabatic energy production, GE , and the baroclinic conversion, CA .

4. CISK Diabatic Forcing

a. Convective Heating Parametrization

As the ascent at fronts is due to the forcing of ageostrophic convergence at low-levels it seems that a reasonable parametrization of convection would depend on this convergence. The CISK type of heating—‘conditional instability of the second kind’—is specified to be proportional to the vertical velocity at a given height, with a predetermined vertical structure. ‘Vertical’, in the semigeostrophic system, may be taken to be geostrophic Z (‘slantwise CISK’, as in CC88) or physical z for upright heating. Specifically the heating is given, following CC88, by,

$$\frac{D\theta}{Dt} \equiv S = \overline{\theta_Z} \epsilon h(Z) w(Z_B), \quad (13)$$

in the slantwise case, where Z_B is the lower level of the heating. The structure function, $h(Z)$, is a specified function of height, normalised such that,

$$\frac{1}{H} \int_0^H h(Z) dZ = 1, \quad (14)$$

where H is the tropopause height and ϵ is the nondimensional parameter controlling the heating magnitude; CC88 cite observational papers which suggest that reasonable values of ϵ for polar lows can be up to 3.0, if surface moisture fluxes are taken into account.

As in CC88, $h(Z)$ is taken to be a triangular profile with peak just below the mid-troposphere at $Z = Z_L$ and zero heating above $Z = Z_T$ or below $Z = Z_B$. In general, these levels are taken, as in CC88, to be $(Z_B, Z_L, Z_T) = (0.1, 0.4, 0.7) \times H$, giving a heating structure that is shifted towards lower levels. If the heating form given by (13) is taken ‘unconditionally’ throughout the flow, there is unphysical diabatic cooling in a column above regions of $w(Z_B) < 0$. It is an advantage of the numerical simulation that ‘conditional’ heating may be invoked, applying (13) only when there is ascent at Z_B .

The specific form of the structure function, $h(Z)$, is important to consider, in that it specifies the heights at which diabatically produced pv anomalies will occur and consequently affects the degree of coupling with the dry baroclinic wave at top and bottom. However, coupling is always likely to be more direct at low levels because heating is defined to be proportional to the vertical velocity at the lower CISK level, Z_B , which will tend to be linked to the positive jet and positive thermal advection, by the rule of thumb given in section 3.2. Note that boundary θ perturbations may be treated conceptually as thin layers of pv perturbation, using Bretherton’s (1966) model. If low level vertical motion is associated with the meridional jets and thermal advection, θ anomalies and pv anomalies are likely to be linked near the lower surface. Positive meridional wind gives positive thermal advection, while the associated ascent and latent heating will give a positive low level pv tendency. Since surface θ and low level pv are dynamically equivalent, the low level wave will be amplified by the CISK. Since, in the CISK parametrization, heating is only directly linked to vertical velocity at low levels, such a direct coupling will not occur in the mid- and upper-levels.

To summarise, briefly, CC88’s results, they found a distinct transition in the behaviour of waves as heating parameter was increased. For low ϵ the modes were structurally similar to the dry wave, with maxima of meridional wind and potential temperature on the boundaries and a baroclinic energy conversion which was dominant over the diabatic conversion. For larger ϵ , greater than around $\epsilon = 1.4$, the diabatic energy conversion

became dominant. In this regime, waves were structurally altered, with the maxima of geostrophic fields determined by the heating boundaries rather than the physical boundaries and wavelengths of the fastest growing solutions were reduced. CC88 also isolated a 'pure CISK' mode, a solution of the CISK problem with zero basic state baroclinicity. This solution does not have a well defined growth rate and is difficult to interpret physically. However, for the conditional heating employed here, such modes have not been found.

5. Normal Mode Computations

As in Joly and Thorpe (1989), numerical 'normal mode' solutions to the various problems discussed are computed, under the SG formulation, using the so-called 'initial value' technique. It is stressed that this method is limited by the inherent nonlinearity of the 'conditional' relationship between heating, S , and vertical velocity, w . A smooth (S, w) relationship may be linearised legitimately about $w = 0$ but the conditional $\frac{1}{2}(w + |w|)$ type of function is not differentiable at $w = 0$ so linearisation is not strictly valid. The process must be seen as the identification of a slowly varying structure of small amplitude; an extension of the smooth heating cases which will be good numerical approximations to the linear normal modes as calculated in CC88. In addition, it is helpful to see these solutions, which are independent of initial perturbation, in tandem with finite amplitude simulations from a specific initial state. Because of the nonlinearity of conditional heating, analytical solutions to the conditional problem are generally intractable, although EFT give a 2-layer solution to a conditionally heated problem.

The initial value method used to evaluate these normal modes is to grow a solution which remains small in amplitude so that the nonlinear terms are kept small. This is achieved by shrinking the solution to small amplitude periodically. The reduction is performed on the geostrophic streamfunction (since no pv perturbation is required for unstable modes) and other quantities are rescaled in conjunction. This method attempts

to find solutions with modal structure in geostrophic streamfunction: the initial perturbation has maximum θ' amplitude of around $10^{-6}K$. Despite the nonlinearity of the conditional heating, in practice the amplitude of modes grows exponentially with time.

As in linear studies, for the small amplitude numerical calculations advection is dominated by basic state terms because the SG system becomes exactly QG in the limit of infinitesimal perturbations. Similarly, M-surfaces, where $M \equiv X = x + \frac{v'}{f}$, become almost vertical as v'_g tends to zero and thus there is no difference between ‘upright’ and ‘slantwise’ CISK in the small amplitude runs.

The simulation of the fastest-growing unconditional mode (figure 1) in which wavenumber, $k = 3.85$ (nondimensionalised with the reciprocal of Rossby radius) and heating parameter, $\epsilon = 2.1$, show that in this case the analytical solutions of CC88 are well reproduced. Figure 2 shows results for the conditionally heated system, using these same parameters.

Although the growth rate, nondimensionalised with $\frac{\overline{U_Z} H}{L_R}$ following CC88, is reduced from $\sigma \approx 1.5$ to $\sigma \approx 1.16$ (figure 3), there is still an unstable mode in which the diabatic conversion is much greater than the wave’s baroclinic energy conversion. In fact, the ratio of integrated diabatic conversion to baroclinic conversion, $\frac{GE}{CA}$, increases from 7.4 in the unconditional case to 11.9 with conditional heating. The reason for this is that as the wave becomes less symmetrical, the baroclinic conversion decreases more rapidly than the diabatic conversion, for given amplitude of the geostrophic fields.

The dominance of the diabatic conversion is increased, despite the fact that in the conditional case pv anomalies are just positive at low levels and just negative aloft. It might be thought that at any level opposite signs of pv anomalies would be needed in order to have a growing solution. However, the zero and positive anomalies may be seen as negative and positive anomalies to an increased mean pv at the given level (in

the sense that the first term in a Fourier decomposition of the pv pattern would be the mean of the pattern).

The conditional mode of figure 2 shows a marked contrast between the upper and lower level patterns. Near the wave steering level, which is close to the upper heating level, the negative pv perturbation is narrow and intense compared to the low level positive anomaly. This is manifested in strong meridional jets aloft; in CC88's results a similar phenomenon was seen. Close to the steering level the pv anomalies advect with the wave and amplify strongly whereas lower down the pv is advected away from the heating region to form a broader and weaker anomaly. It should be noted here that although the pv tendency in the computed modes is piecewise constant with height, the zonal shear of the pv means that the induced anomalies have a height structure.

The low level jet in this simulation is elevated above the ground; another indication of the significance of diabatically induced pv and θ anomalies in this parameter regime. It is the cutoff of pv with height that closes off the jet. Similarly, the boundary θ anomalies are relatively weak compared to the interior anomalies.

In the conditional solution, the lower level positive jet is more intense and more localised than the region of negative meridional flow. The short lengthscale of this jet is much less than a Rossby radius and lies on the eastern flank of the low level pv anomaly. This may be understood by interpreting the pv pattern as being directly linked to the relative vorticity, with $\zeta = f + v_x \propto q$, and noting that the integral of relative vorticity along a horizontal wavelength is perforce zero. This qualitative form for relative vorticity is confirmed in the model output and the jet lies between the maximum and minimum of the relative vorticity field. Thus the x-dimension of the low level jet is determined by the horizontal scale of the zonal pv gradient on which it lies. The jet seems to be horizontally confined by the pv gradient. In contrast, the negative jet is broader and weaker, as the western side of the pv field has a shallower gradient.

The vertical velocity field of the conditional wave shows that the strong diabatic forcing of the S-E equation produces a dipole in $\frac{\partial S}{\partial X}$ which generates an overturning cell on each side of the updraught. Indeed, the downward velocity shown in figure 2 reaches almost 50% of the magnitude of the updraught: this is relatively large when compared with conditional simulations using ThEm heating, such as EFT. The downdraught to the west is the weaker of the two because of the positive upper jet in this region, which will tend to force upward motion.

It is significant that the growth rate, phase speed and minimum updraught width curves of figure 3 are all remarkably flat, from wavenumbers of order 2.0 to around 4.5, at which the growth rate starts to tail off. Within this range of wavenumbers the dynamics of the active region of the flow, in the vicinity of the updraught, are almost unchanging. It seems that the broader downdraught region has little influence on the development of the wave, until around wavenumber 4.0. At this wavenumber the horizontal extent of the periodic domain is reduced to a value close to the Rossby radius of deformation, so that adjacent waves interact and reduce the growth rate. The pv anomalies of adjacent waves, whose influence decreases over a distance of order of the Rossby radius, interact more strongly at higher wavenumber and the particular nature of the individual waves is altered. For the longer wave modes, interaction between successive waves seems to be so weak as to be irrelevant.

With the observation that it appears only to be the local dynamics which matter to the long-wave conditional CISK modes, the active regions may be seen as exponentially growing analogues of solitary waves, independent of each other provided they are sufficiently far apart. The dynamics may be interpreted in terms of the pv tendency at low levels. The positive pv anomaly close to the heating base-height, Z_B , tends to induce poleward flow on its eastern flank, by the mechanism described above. This positive meridional jet may be interpreted as inducing upward motion, through the S-E equation and the association of w with thermal advection; this gives a column of

heating. The heating provides a positive pv tendency to the east of the pv anomaly, as a Rossby wave would through meridional advection, which gives the wave its propagation. However, advective effects are not negligible, as may be seen from the intensity of the upper negative pv anomaly, which advects approximately at the same speed as the wave propagates. The analogy with a dry Rossby wave is expanded in section 6.

Solutions at smaller wavenumbers than $k = 2.0$ are difficult to compute numerically as more than one mode appears in the domain. This is not necessarily to say that there is a dominant shorter wavelength; rather that the waves are independent and may grow out of numerical noise, provided they are separated by at least a Rossby radius.

The independence of the conditional modes to overall wavelength is peculiar to this system. The unconditional modes of CC88 show generally sharp peaks in growth rate with wavenumber. Furthermore, the conditionally heated modes computed in Joly and Thorpe (1989) for the ThEm scheme also show peaks in growth rate, with roughly the same functional shape as in the dry problem, as wavenumber is varied. The ThEm system sets heating as dependent on local conditions at all levels and its dynamics depend on pv anomalies at upper and lower levels—in this way it is much more akin to a dry baroclinic wave in which the role of the boundaries is crucial. In the CISK system, only the lower-level pv pattern feeds back directly on the heating. Consequently, the wave is much less similar to the canonical Eady wave. With the dominant CISK, the role of the basic state baroclinicity is to provide the mechanism for upward motion, through the S-E equation.

1) SENSITIVITY TO HEATING AMPLITUDE

Since the conditionally heated CISK modes for high value of heating parameter seem to be only weakly dependent on overall wavelength in their growth rate, phase speed and local structure, the behaviour of waves in this parameter regime may be determined in a rather general way. One structure, for given large epsilon, will specify the behaviour

of the system for a range of overall wavenumbers, provided the waves have the ‘solitary’ behaviour observed.

Figure 4 shows the behaviour of the parameters plotted in figure 3 as the heating parameter, ϵ , is varied. For high values of this parameter the modes exhibit the solitary behaviour described above and the computed values of growth rate, phase speed and local structure are independent of wavelength; at lower ϵ the waves, like the dry mode, vary with wavelength. A nondimensional wavenumber of $k = 3.0$ was taken to calculate these modes. As in the unconditionally heated case, the phase speed curve shows that the nature of the solutions changes markedly, at around $\epsilon = 1.7$ here, as the transition from baroclinic to moist-dominated solutions occurs.

The qualitative form of the dispersion relation for the conditional modes is shown in figure 5, for heating parameter, $\epsilon = 1.0$. This figure shows that the wave has significantly different behaviour for lower heating parameter than observed at $\epsilon = 2.1$. The dispersion relation has a distinct local maximum growth rate around wavenumber $k = 2.5$. As might be expected, from the energy conversion terms there is no evidence that moisture dominates the flow.

In the regime of dominant heating it can be seen that the phase speed and growth rate increase with ϵ while the updraught width falls. The nondimensionalisation of CC88 shows that the only free parameters in the solution are the wavenumber, k , the heating parameter, ϵ , and the heating structure. Since it seems that in these cases the overall wavenumber is unimportant, provided it is low enough, the only parameters governing the solitary modes are ϵ and heating profile. Given these parameters,

$$L \propto L_R, \quad (15)$$

$$c \propto H \frac{du_g}{dZ}, \quad (16)$$

$$\sigma \propto \frac{H \frac{du_g}{dZ}}{L_R}, \quad (17)$$

where L_R is the Rossby radius.

2) SENSITIVITY TO HEATING PROFILE

CC88 comment on the way in which unconditionally heated normal modes are modified by varying the vertical profile of heating structure. In general, reducing the height of the heating levels produces faster growth and shorter-wave modes. This may be interpreted as being due to an enhanced coupling between the dry boundary Rossby wave and the moisture induced pv wave. CC88 state that the lower pv maximum will tend to increase low-level convergence and thus increase the heating. The phase speed of modes, however, is marginally reduced with lowered heating levels. This may be due to the low-level pv anomalies descending into a region of faster negative advection. This effect may also account for the narrowing of fastest-growing modes.

6. The Diabatic Rossby Wave

In considering the dry Eady wave, much understanding can be gained by interpreting the system as the interaction between boundary Rossby waves. It was mentioned in the last section how the pv tendency due to diabatic heating acts in a similar manner to the meridional advection of pv in a Rossby wave: here this will be explored in more detail. The dynamics will be interpreted as a 'diabatic Rossby wave' at the lower level of the heating. This analysis will lead to a simple prediction for the propagation speed of the disturbance.

The mechanism of the wave as it occurs in the conditional CISK modes may be seen schematically in figure 6: meridional wind gives thermal advection which yields forcing of upward motion, giving diabatic heating and a pv source. Interpreting the pv anomalies, which are generated by a vertical gradient of heating and consequently a tendency in the static stability, as vorticity anomalies is possible because of the balance implicit in the SG equations. The ageostrophic motion acts to maintain this balance so the propagation may be seen in ageostrophic terms. The vorticity at the lower heating

level gives thermal advection on its eastern flank, which leads to upward motion and heating. The upward motion induces vortex stretching and increases the vorticity to the east of the lower, positive anomaly, giving propagation as in the previous interpretation.

A scale analysis of the diabatic wave may be made by using a one dimensional model of the low level pv structure with zonal distance, at height $Z = Z_B$. For an unconditional heating parametrization, an exact proportionality between meridional wind, vertical velocity and pv tendency, as implied by (9), would give a perfect analogue of a Rossby wave. However, the dynamics of a conditionally heated system have been shown to behave rather differently and the scale analysis given here will focus on the propagation of the positive meridional jet which lies on the eastern flank of the low level pv anomaly.

If the magnitude of the pv anomaly is Δq , with a meridional jet of width L on its eastern edge, the meridional jet amplitude, V_B , scales as,

$$V_B \sim \frac{L}{4} \frac{\rho \Delta q}{\theta_Z} \quad (18)$$

The factor of 4 in the denominator of (18) arises from the simplest scaling of relative vorticity with the change in meridional wind. On each side of the jet, the relative vorticity scales as $\frac{2V_B}{L}$ so the amplitude of the absolute vorticity anomaly, $\Delta\zeta$, scales as twice this value. Approximating $\Delta\zeta \sim \frac{\rho \Delta q}{\theta_Z}$ gives (18). An unconditional wave, with sinusoidal profile of pv anomaly, would have a different constant in this equation but the basic form would be the same.

The meridional jet is linked with ascent in the presence of synoptic forcing, as can be seen from (9). This ascent gives diabatic heating which leads to a positive pv tendency in the region of the jet and a negative tendency aloft. The pv tendency at Z_B can be found by substituting (13) into (3):

$$\dot{q} = \frac{\zeta}{\rho} \overline{\epsilon \theta_Z} \frac{\partial h}{\partial Z} w(Z_B) \quad (19)$$

Using the approximate relationship (9) and recalling that $S(Z_B) = 0$, the pv tendency at Z_B becomes,

$$\dot{q} \sim 2\epsilon \frac{f}{\rho} \frac{\partial h}{\partial Z} V_B(-\overline{\theta_Y}) \quad (20)$$

The r.h.s. may be seen to be equivalent to pv advection, with an equivalent 'diabatic pv gradient' given by,

$$\left(\frac{\partial q}{\partial Y} \right)_{equiv} = 2\epsilon \frac{f}{\rho} \frac{\partial h}{\partial Z} (-\overline{\theta_Y}) \quad (21)$$

For the parameters used in the model described here, with $\epsilon = 2.1$, this counterpart of the meridional pv gradient for a traditional Rossby wave is of order $-3 \text{ PVU}(1000\text{km})^{-1}$. This can be compared to that implied by the latitudinal variation of Coriolis parameter, which implies a meridional pv gradient of order $+0.06 \text{ PVU}(1000\text{km})^{-1}$.

Substituting (18) in (20) gives,

$$\dot{q} \sim L \Delta q \left(\frac{\epsilon f \frac{\partial h}{\partial Z} (-\overline{\theta_Y})}{2\theta_Z} \right) \quad (22)$$

For a steady state model of the propagation of a pv step in which the growth of the system is ignored, the phase speed, c , relative to the flow at the level of the pv anomaly, $Z = Z_B$, may be estimated by equating $c\Delta q$ with $\dot{q}L$, to give,

$$c \sim \left(\epsilon H \frac{\partial h}{\partial Z} \right) \left(\frac{L}{L_R} \right)^2 \overline{U_Z} H \quad (23)$$

In practice, the heating factor $\epsilon \frac{\partial h}{\partial Z}$ would need to be estimated in order to evaluate the phase speed of such a convective pv step. Note that the relation (23) is independent of the amplitude of the pv anomaly (as may be expected for a modal solution) but depends on the scale of the pv gradient: (23) represents a form of dispersion relation and satisfies to simple scaling relationship of (16). Letting the values of the parameters in (23) be as prescribed in the numerical simulations and taking $L \sim 250 \text{ km}$ from figure 2 of the results gives a phase speed relative to the flow at Z_B of $c \sim 15 \text{ ms}^{-1}$.

Given the link between geostrophic forcing and the pv tendency implied by (9), the pv equation becomes isomorphic to that of a Rossby wave on a meridional pv gradient. The diabatic equivalent to this meridional gradient of pv has the opposite sign from that for Rossby waves, given an equatorward temperature gradient, so diabatic waves propagate in an eastward direction. Since the control of heating is at the lower level, it is natural to view the Rossby wave analogy at this height, independent of upper behaviour.

It has been indicated that, depending on the amplitude and structure of the convective heating, the diabatic ‘gradient’ can be relatively large in magnitude and is expected to dominate over pv advection in some cases. In the atmosphere, however, it is important to appreciate that the significant diabatic pv tendency due to convection will only be positive, at low levels, because of the failure of evaporative processes to couple with the dynamics of the frontal system (as in Parker and Thorpe, 1994). Consequently, this theory is applicable to a single pv step with a positive pv tendency on its flank rather than a train of waves, with negative and positive heating at low levels, as occurs in the unconditional parametrization.

No attempt has yet been made in this scale analysis to account for the interaction of the wave at $Z = Z_B$ with the upper level behaviour. Snyder and Lindzen (1991) discuss how these levels interact in the unconditionally heated case to produce an instability. For growing, conditionally heated solutions, it is important to note that the upper level minimum of pv must be located almost directly above the low level jet, within

the column of diabatic heating, since there are no diabatic sources outside the heating region. As a consequence, this negative anomaly induces upper level jets, as seen in figure 2, which will interact with the lower level flow to increase the low level jet (and consequently the pv tendency) to the west, closer to the pv maximum. This is a way in which interaction with the upper level can increase the growth of the front. Since there is no coupling between meridional flow and heating at upper levels it is not reasonable to consider the upper level structure in terms of an analogue of a Rossby wave. The vertical interaction will, however, mean that the phase speed of the coupled system is related to but not equal to that given by (23).

7. Large Amplitude Solutions

Nonlinear computations require a specific initial state. A criticism of the technique of simply studying fastest-growing normal modes has been that the initial development of a perturbed flow may be dominated by time-dependent structures which maximise their component of the fastest-growing mode. For example, the small amplitude development of a dry Eady wave from a general initial state may be dominated by non-modal structures, as shown by Farrell (1984). Computation of such time-dependent structures would be difficult in the inherently nonlinear conditionally heated flow, but a realistic study may be made by considering nonlinear growth from particular initial forms. Here, results will be described in which the initial structure is that of the numerically computed normal mode.

In addition to the occurrence of boundary singularities, failure of the SG solution may occur in the interior of the domain if diabatic processes are involved in the nonlinear system and pv becomes negative. It can be shown that the ThEm heating scheme will not ordinarily produce negative pv (Parker, 1993) but CISK heating does not obey such constraints: in the CISK case, interior pv may reach zero before any boundary singularity is achieved. In this work, no consideration of flows at negative pv is to be made: this would involve the study of symmetric instability and turbulent processes.

The role of turbulent mixing in modifying a pv distribution can be a perplexing one: Thorpe and Rotunno (1989) show that mixing of momentum and potential temperature need not lead to a smoothing of the pv field and there is a possibility of upgradient mixing of pv.

a. Moist Normal Mode Initialisation

The system was integrated using a numerically computed normal mode as the initial condition, rescaling the mode so that the maximum perturbation in potential temperature was about $1K$.

For simplicity, solutions for upright heating only are shown, in figure 7, at the termination of the integration. The upper level pv has decreased to zero and the inversion from geostrophic coordinates fails beyond this, despite the fact that the geostrophic field of meridional wind is relatively weak, with no singularities.

The ageostrophic flow shows strong downward velocity to the flanks of the heating region: the amplitude is of the same order as that of the upward flow. These downdraughts are forced by the strong dipole on the r.h.s. of the S-E equation (6) due to the horizontal gradient of diabatic heating. The implications of this are that strong adiabatic warming and consequent lowering of the relative humidity of the air is to be expected to both sides of the heating region. This agrees qualitatively with observations that such convective fronts can have sharp edges to the cloud when seen from a satellite image. As in the linear modes, the stronger of the two downdraughts is to the east of the updraught.

Qualitatively, both the upright and slantwise routines retain the essential structure of the normal mode, when integrated at larger amplitude. There is a positive low-level jet on the eastern flank of the positive pv anomaly. Above this, the negative pv anomaly is more intense and localised, although there is evidence of the role of ageostrophic advection in distorting the pv pattern. The upper pv anomaly is flanked by relatively strong jets.

b. Observational Evidence

Figure 8 shows fields from the U.K. Meteorological Office Unified Limited Area Model analysis for 18Z on 12 November 1991. The coupling between along-front wind and diabatic heating is indicated by the fact that the column of high relative humidity lies above the low level jet, which lies on the flank of a positive potential vorticity anomaly, as in the models described here. It should be recalled that this behaviour relies on the existence of an along-front temperature gradient to provide thermal advection. As in the wave-CISK model, the upper level jet is much stronger than the low level jet. It can also be seen that the upper regions of the column of high humidity are associated with low potential vorticity, again in accordance with the model. In particular, the fact that the humid air at upper levels lies on the low pv anomaly rather than the along-front jet is an indication that these observations accord more closely with the convective model of heating than the ThEm model. It should be recalled that in the theoretical CISK model, the intensity and localised nature of the upper potential vorticity minimum was determined by the steering level of the wave.

At upper levels there is a strong positive potential vorticity anomaly in these observations, linked with a marked change in tropopause height: the tropopause is not well represented in the modelled waves, which use a rigid lid. However, the drawing down of stratospheric potential vorticity may be seen as being due to the intense downward vertical motion as modelled in the conditional convective modes. This may be again reflected in the low relative humidity of this region.

8. Summary and Discussion

In this paper, conditional baroclinic wave-CISK modes have been constructed as a natural extension of the work of Craig and Cho (1988). These modes exhibit behaviour which is characteristic of 'solitary' systems, in that the dynamics of the active frontal region are independent of the far field. As such, they are conceptually different in their dynamics to the 'dry' frontal paradigm of a baroclinic wave. Here we coin the term

'convective frontogenesis' for this mechanism. Snyder and Lindzen (1991) note, for an unconditionally heated wave, that the diabatic source of pv can act as a 'dynamical surrogate' for large scale pv gradients. Here, this interpretation has been extended and the essential behaviour has been viewed in terms of a 'diabatic Rossby wave'. The mechanism of this wave has been shown schematically in figure 6, and a steady state model of the propagation of a pv step has been constructed.

The solitary modes described above exhibit dominant moist processes, independence to the flow in the far field and low level control of the dynamics. These are all properties normally associated with squall lines rather than synoptic baroclinic systems. It should be noted, however, that there are other aspects of these waves which do not fit the squall line model, such as the lack of feedback through evaporative cooling (there is no explicit cooling in this model, although this can be considered; see Parker and Thorpe (1994)) and the absence of a marked cold pool: both are crucial to the conceptual squall line picture.

The importance of these waves is that they do share properties of both the synoptically-forced model and the squall line model. In this respect they represent a bridge between the two areas of study. These waves point to the fact that convection can modify a larger scale flow so as to make the moist processes dominant—the structure of these modes is far removed from that of a dry wave, as is the manner of development. Similarly, they show how the balanced dynamics are sufficient to produce a flow with many of the observed properties of a squall line: it would be reasonable to expect that in more conventional squall line systems these dynamics will still play an important role.

Since, in this CISK model, control of the wave seems to be dominated by the dynamics at the lower heating level, this system potentially couples more directly with low level phenomena such as a cold pool. It is less difficult to see, in a model such as this, why synoptic frontal speeds can concur with the gravity current speed of the cold front, than it is in more conventional balanced models. In nature, a coupling

between gravity current processes and the modified (diabatic) Rossby wave at the lower heating level may occur. In models where the conventional upper and lower Rossby wave patterns seem to determine the wave propagation, such as the dry Eady wave, a link with low level unbalanced dynamics is hard to imagine.

Fovell (1991) suggested that the influence of the Coriolis parameter and a balanced basic shear in the basic state may be to prolong the existence of a squall line. The solitary modes described here indicate that squall lines may be able to excite growing modes of a baroclinic atmosphere, which are, in this model, locally forced.

The links of the diabatic Rossby wave mechanism depend on the feedback between thermal advection and vertical motion. In principle, other assumptions about the physics of the system could be made. For instance, a feedback with an assumed Ekman layer could be invoked, in which the heating was dependent on vorticity at the lowest levels. In this case, the pv tendency would lie closer to the actual low level pv anomaly, associating pv directly with vorticity, and the steering level of the wave would be expected to be much closer to the ground. Observational evidence has been presented here indicating that the dynamics described in the inviscid model with a free-slip boundary condition can be dominant in the atmosphere, but other cases can exist in which the steering level is lower down (Andre-Charles Letestu, personal communication).

The diabatically dominated modes have been termed 'solitary' in order to highlight their localised nature and the fact that their structure is robust to changes in overall wavelength. The wave-CISK solutions have been constructed as small-amplitude, 'linear' waves in which nonlinear advection is negligible, although there is nonlinearity in the conditional heating. However, although they retain their shape, they are exponentially growing. It is not clear how larger-amplitude versions would ultimately behave because of the difficulty of parametrizing the effect of negative pv. It is possible that limiting factors on the growth of these waves (such as an upper limit on the amplitude of the

heating) could give behaviour in which the pv resembled a smoothed step-function in the horizontal, with the convective band leaving high pv at low levels in its wake.

The localised frontal structure that this model describes is dominated by latent heat release in the sense that the frontogenesis is determined by gradients of heating rather than by horizontal shear forcing. However, the constraint of along-front geostrophy, which is a fundamental support of frontogenesis theory, requires that the larger-scale forcing, by the shear and along-front temperature gradient, exists even if it is of a relatively small magnitude. It acts as a catalyst, triggering low level frontal convergence which leads to convection. This produces diabatic forcing of frontogenesis which far outweighs the original catalyst. The notion of convective frontogenesis therefore arises as a dominant mechanism in midlatitude storms.

Acknowledgements. The authors would like to thank George Craig for many useful discussions regarding this problem and Huw Davies for some pertinent criticism. Thanks also to Andre-Charles Letestu for producing the observational figures and Ken Spiers for drawing figure 6. Doug Parker received an NERC research studentship whilst undertaking this work.

REFERENCES

- Bannon, B.R., 1986, 'Linear development of quasi-geostrophic disturbances with condensational heating', *J. Atmos. Sci.*, **43**, 2261-2274.
- Bretherton, F.P., 1966, 'Critical layer instability in baroclinic flows', *Quart. J. Roy. Meteor. Soc.*, **92**, 325-334.
- Browning, K.A. and Harrold, T.W., 1970, 'Air motion and precipitation growth at a cold front', *Quart. J. Roy. Meteor. Soc.*, **96**, 369-389.
- Craig, G.C. and Cho, H-R, 1988, 'Cumulus heating and CISK in the extratropical atmosphere. Part I: Polar lows and comma clouds', *J. Atmos. Sci.*, **45**, 2622-2640.
- Cram, J.M., Pielke, R.A. and Cotton, W.R., 1992, 'Numerical simulation and analysis of a prefrontal squall line. Part I: Observations and basic simulation results', *J. Atmos. Sci.*, **49**, 189-208.
- Cram, J.M., Pielke, R.A. and Cotton, W.R., 1992, 'Numerical simulation and analysis of a prefrontal squall line. Part II: Propagation of the squall line as an internal gravity wave', *J. Atmos. Sci.*, **49**, 209-224.
- Eady, E.T., 1949, 'Long waves and cyclone waves', *Tellus*, **1**, 33-52.
- Emanuel, K.A., Fantini, M. and Thorpe, A.J., 1987, 'Baroclinic instability in an environment of small stability to slantwise moist convection. Part I: Two-dimensional models', *J. Atmos. Sci.*, **44**, 1559-1573.
- Farrell, B.F., 1984, 'Modal and non-modal baroclinic waves', *J. Atmos. Sci.*, **41**, 668-673.
- Fovell, R.G., 1991, 'Influence of the Coriolis force on two-dimensional model storms', *Mon. Wea. Rev.*, **115**, 606-630.
- Garner, S.T. and Thorpe, A.J., 1992, 'The development of organised convection in a simplified squall-line model', *Quart. J. Roy. Meteor. Soc.*, **118**, 101-124.
- Gill, A.E., 1982, 'Atmosphere-Ocean Dynamics', Academic Press, New York.

- Hobbs, P.V. and Persson, P.O.G., 1982, 'The mesoscale and microscale structure and organisation of clouds and precipitation in midlatitude cyclones. Part V: The substructure of narrow cold-frontal rainbands', *J. Atmos. Sci.*, **39**, 280-295.
- Hoskins, B.J., 1974, 'The role of potential vorticity in symmetric stability and instability', *Quart. J. Roy. Meteor. Soc.*, **100**, 480-482.
- Hoskins, B.J., 1975, 'The geostrophic momentum approximation and the semi-geostrophic equations', *J. Atmos. Sci.*, **32**, 233-242.
- Hoskins, B.J. and Bretherton, F.P., 1972, 'Atmospheric frontogenesis models: mathematical formulation and solution', *J. Atmos. Sci.*, **29**, 11-37.
- Hoskins, B.J., McIntyre, M.E. and Robertson, R.W., 1985, 'On the use and significance of isentropic potential vorticity maps', *Quart. J. Roy. Meteor. Soc.*, **111**, 877-946.
- Joly, A. and Thorpe, A.J., 1989, 'Warm and occluded fronts in two-dimensional moist baroclinic instability', *Quart. J. Roy. Meteor. Soc.*, **115**, 513-534.
- Lafore, J-P., and Moncrieff, M.W., 1990, 'Reply to Rotunno *et al.* (1990)', *J. Atmos. Sci.*, **47**, 1034-1035.
- Meischner, P.F., Bringi, V.N., Heimann, D. and Holler, H., 1991, 'A squall line in southern Germany: kinematics and precipitation formation as deduced by advanced polarimetric and Doppler radar measurements', *Mon. Wea. Rev.*, **115**, 678-701.
- Parker, D.J., 1993, 'The interaction of moist processes with frontal systems', PhD Thesis, University of Reading.
- Parker, D.J. and Thorpe, A.J., 1994, 'The role of snow sublimation in frontogenesis', submitted to *Quart. J. Roy. Meteor. Soc.*
- Snyder, C. and Lindzen, R. S., 1991, 'Quasi-geostrophic wave-CISK in an unbounded baroclinic shear', *J. Atmos. Sci.*, **48**, 78-86.
- Thorncroft, C.D., Hoskins, B.J. and McIntyre, M.E., 1993, 'Two paradigms of baroclinic-wave life-cycle behaviour', *Quart. J. Roy. Meteor. Soc.*, **119**, 17-56.

- Thorpe A.J. and Clough, S.A., 1991, 'Mesoscale dynamics of cold fronts: structures described by dropsoundings in FRONTS 87', *Quart. J. Roy. Meteor. Soc.*, **117**, 903-941.
- Thorpe, A.J. and Emanuel, K.A., 1985, 'Frontogenesis in the presence of small stability to slantwise convection', *J. Atmos. Sci.*, **42**, 1809-1824.
- Thorpe, A.J. and Rotunno, R., 1989, 'Nonlinear aspects of symmetric instability', *J. Atmos. Sci.*, **46**, 1285-1299.

Figure Captions

FIG. 1. The numerically computed slantwise CISK mode with unconditional heating at wavenumber 3.85 (wavelength 1,900 km), $\epsilon = 2.1$, to compare with the analytical solution of Craig and Cho (1988). In this and subsequent figures, SI units are used except for vertical velocity in $cm\ s^{-1}$ (amplitudes are arbitrary in this case, for the modal structure). ‘STEP’ refers to the contour interval and contours with negative values are dotted.

FIG. 2. CISK mode with conditional heating. Wavenumber 3.85 (wavelength 1,900 km), $\epsilon = 2.1$. The intense upper pv anomaly lies on the wave steering level, while the low level meridional jet lies on the flank of the positive pv anomaly, as discussed in the text.

FIG. 3. The behaviour of growth rate, σ (solid line), phase speed, c , relative to the mid-level (dashed line), and minimum width of updraught (dotted line) with nondimensional wavenumber, for conditionally heated wave-CISK modes; σ and c are nondimensionalised by $\frac{U_Z H}{L_R}$ and $10 \times U_Z H$ respectively, while the width is scaled by 100km. Heating parameter, $\epsilon = 2.1$. An approximation to the growth rate curve of CC88, for unconditional heating, is also given for comparison (dash-dotted). The fastest growing dry Eady wave has growth rate $\sigma = 0.31$.

FIG. 4. The variation of phase speed, c , growth rate, σ , and updraught width (scaled by 300km) with heating parameter for the conditionally heated CISK modes. The transition between ‘baroclinic’ and ‘diabatic’ regimes is around $\epsilon = 1.7$, close to that of the unconditional case.

FIG. 5. A numerical approximation to the dispersion relation for the conditional CISK modes for heating parameter $\epsilon = 1.0$.

FIG. 6. Schematic representations of the dynamics of the diabatic Rossby wave. Here L is the horizontal scale of the jet on the eastern side of the pv anomaly. (a) The poleward jet (marked \times) associated with the low level pv anomaly gives positive thermal advection, leading to upward motion and diabatic heating. (b) This diabatic heating leads to a pv tendency to the east of the low level pv anomaly. (c) A comparison between the dynamical processes involved in the diabatic wave and the classical Rossby wave, linking meridional advection with the pv tendency.

FIG. 7. Fields of pv, meridional wind and vertical velocity (in K per day) for the nonlinear upright CISK waves initialised from a normal mode of the problem. Heating parameter, $\epsilon = 2.1$, wavenumber $k = 3.0$ (wavelength $\approx 2,500$ km).

FIG. 8. Analysed fields of (a) along-front wind (in ms^{-1}), (b) relative humidity (%) and (c) dry potential vorticity (in PVU) on a cross section through a front lying across Southern England. The column of high relative humidity occurs directly above the low level jet, as in the conditional wave-CISK simulations. This low level jet is less intense than the upper level wind maximum, again agreeing with the theoretical modes. It can be seen that the upper level minimum of pv seems to be directly linked with the upper edge of the column of high humidity, as in the modelled convective front.

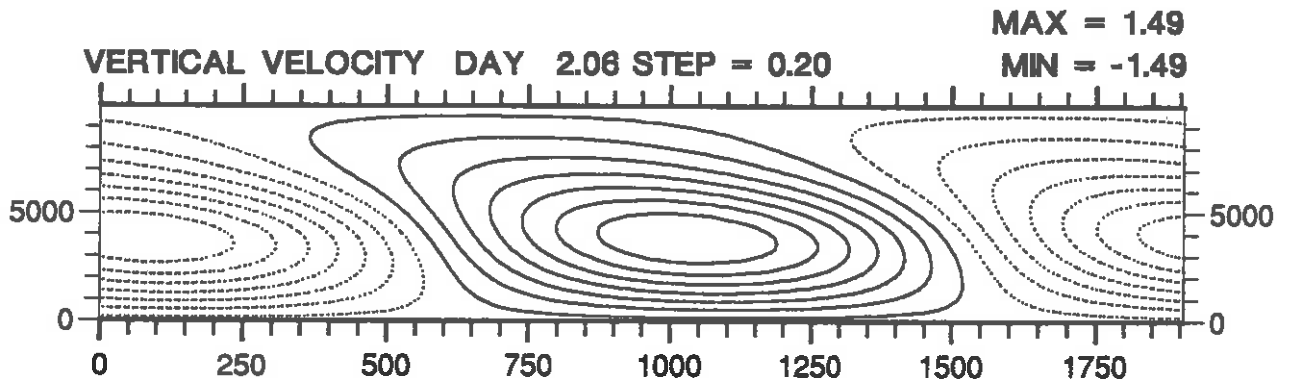
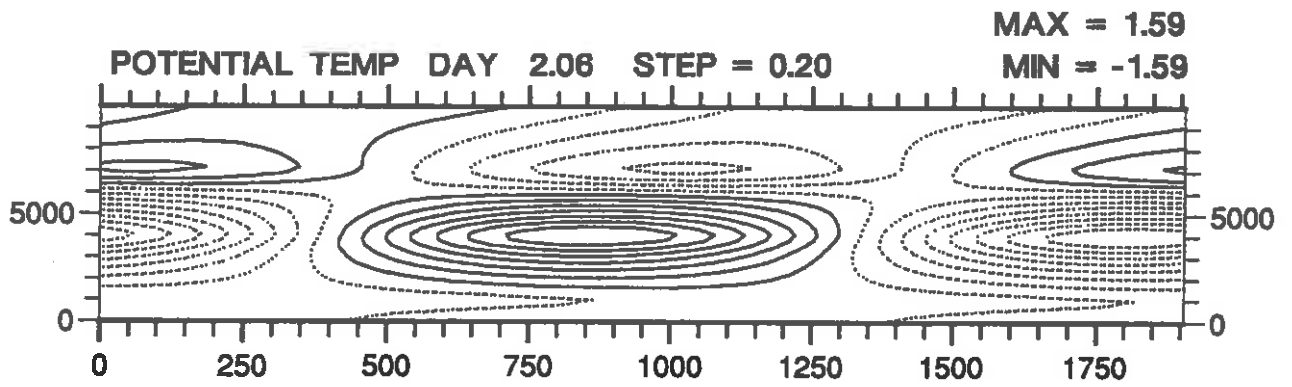


Figure 1

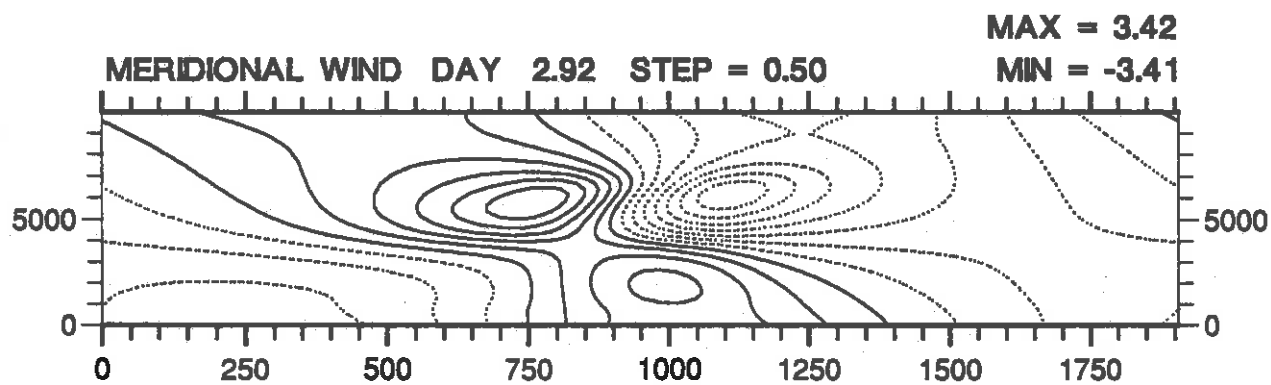
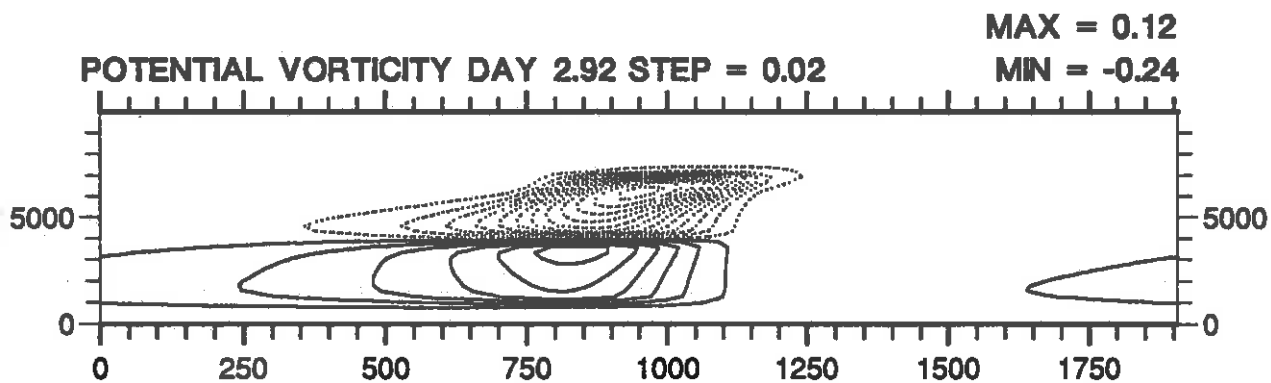


Figure 2 ...

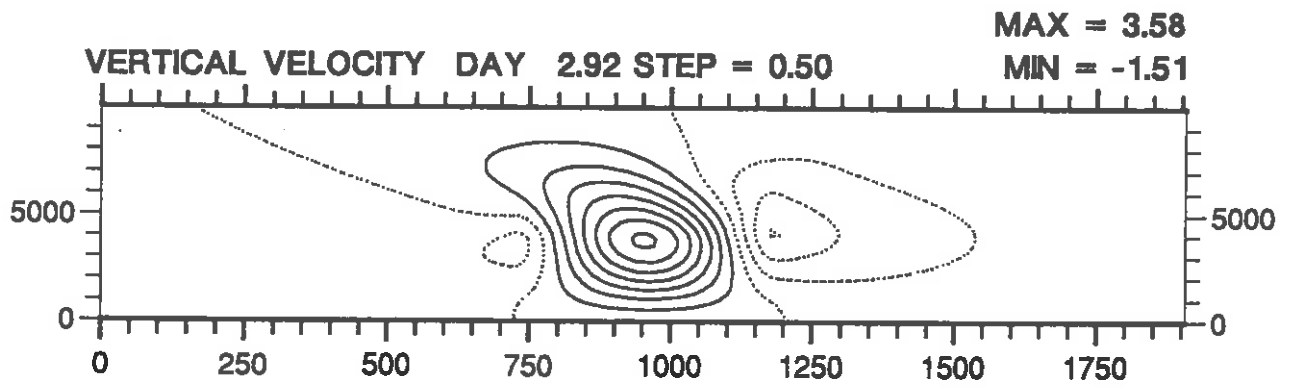
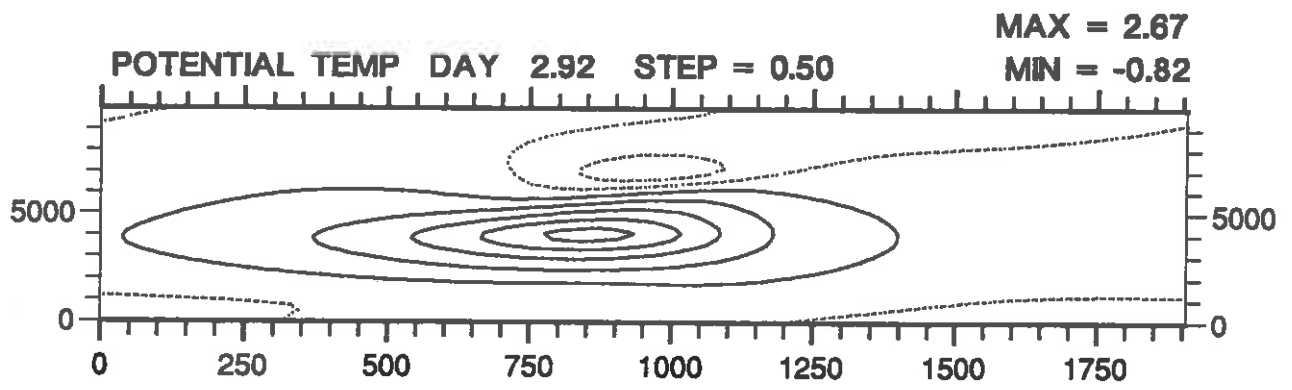


Figure 2

(2/2)

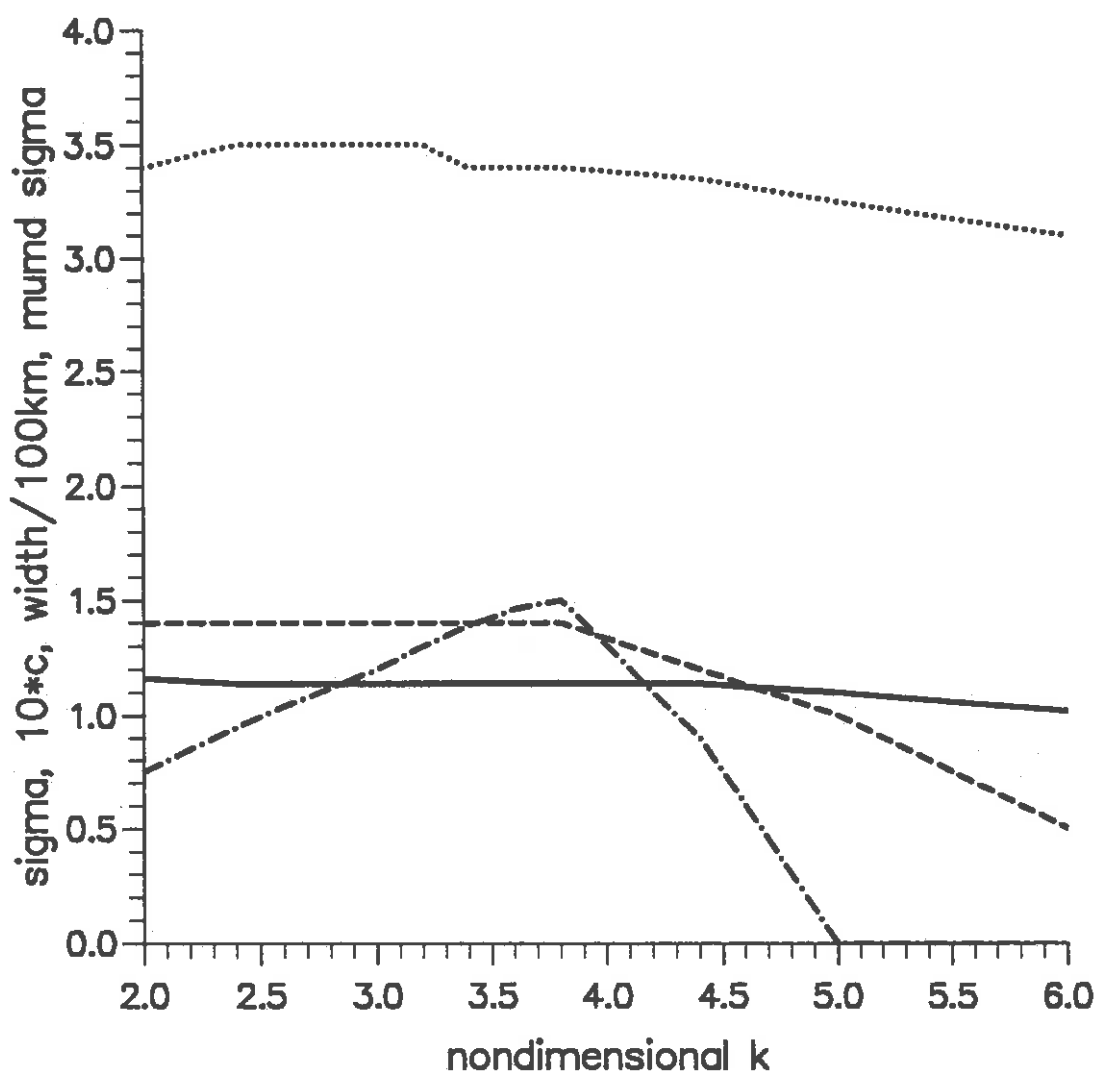


Figure 3

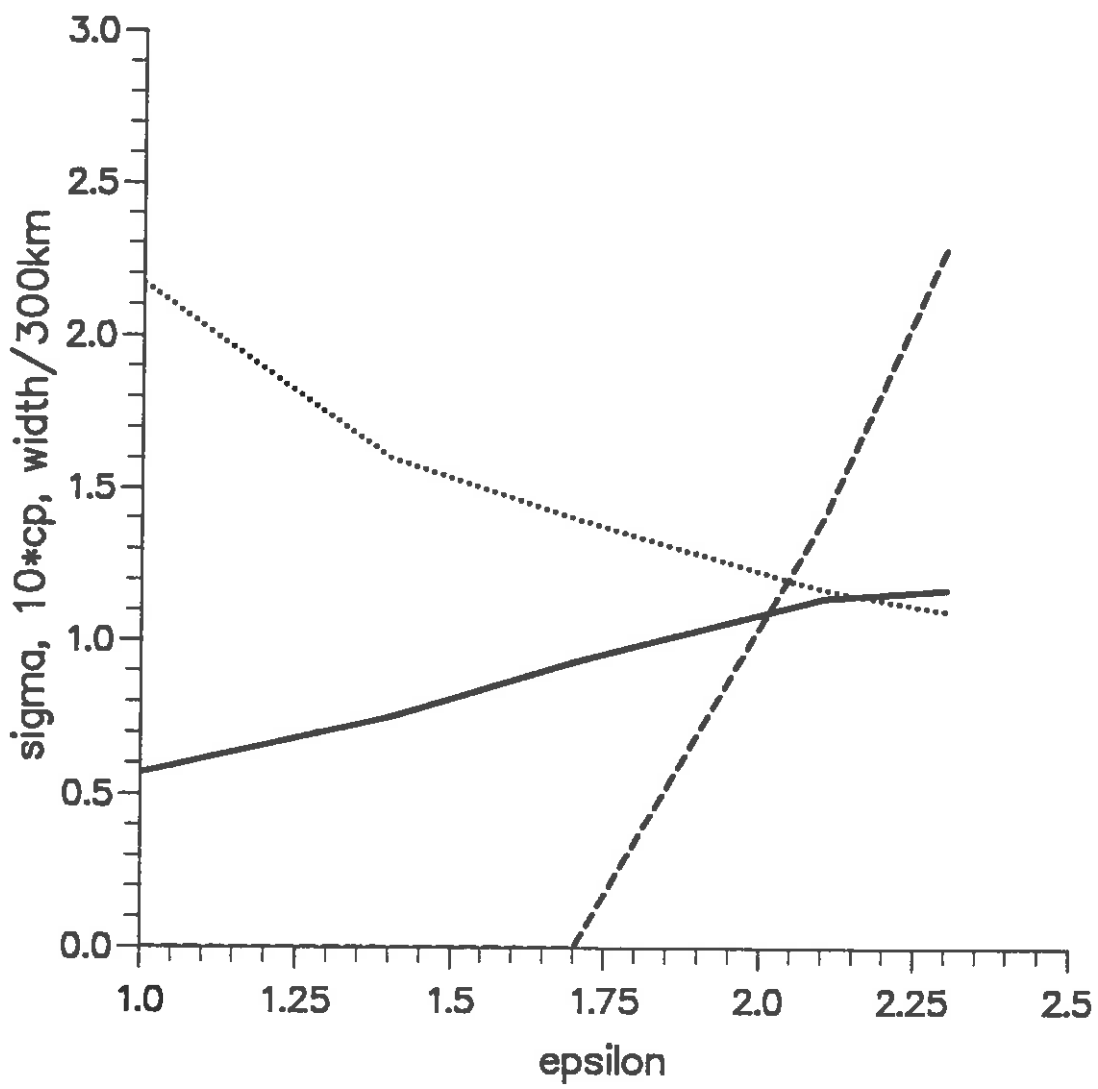


Figure 4

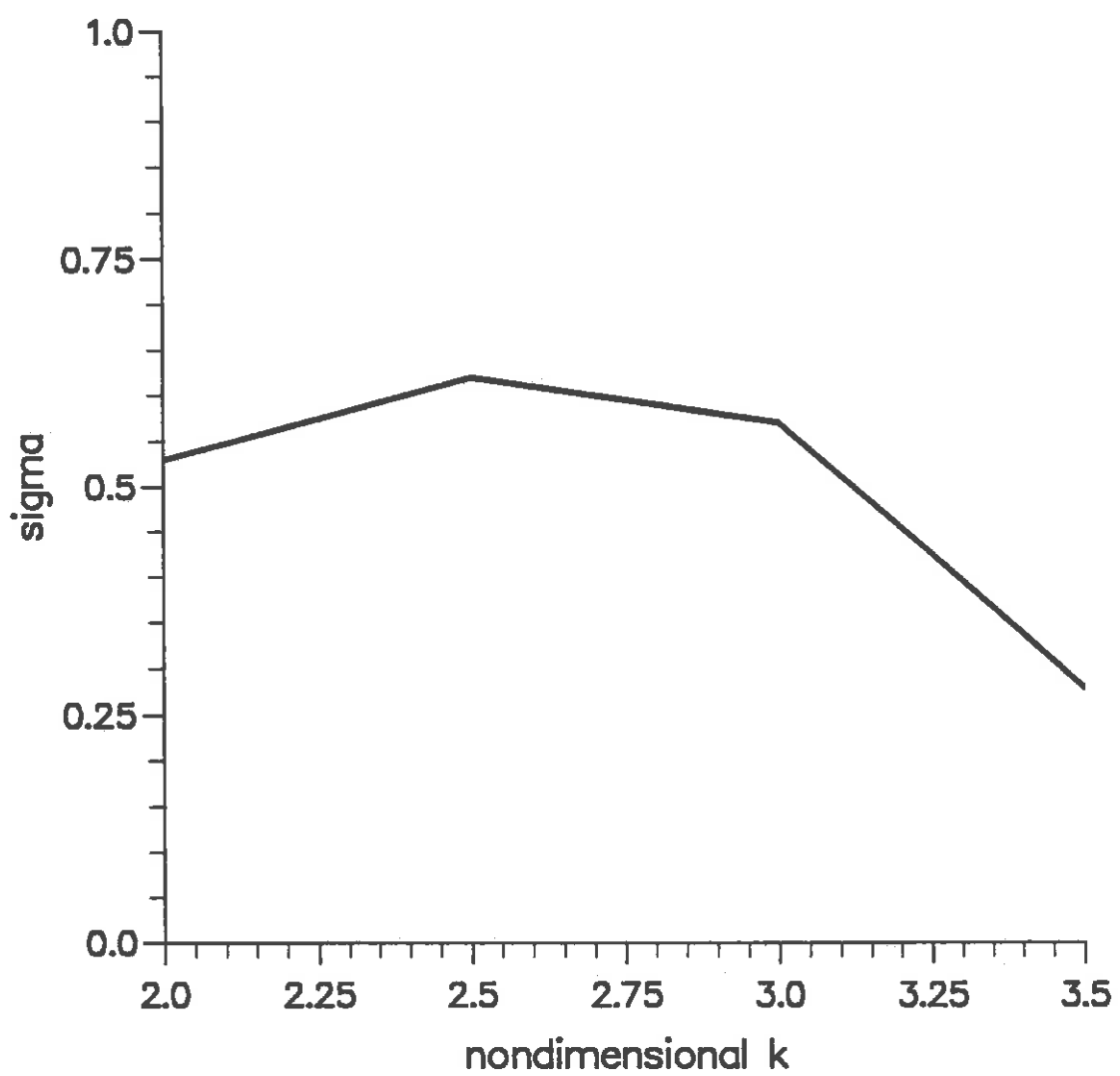


Figure 5

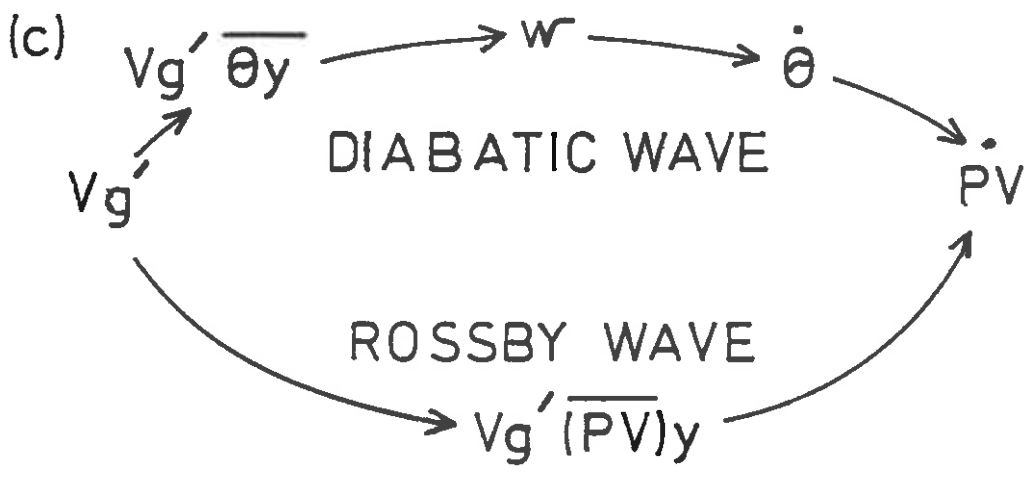
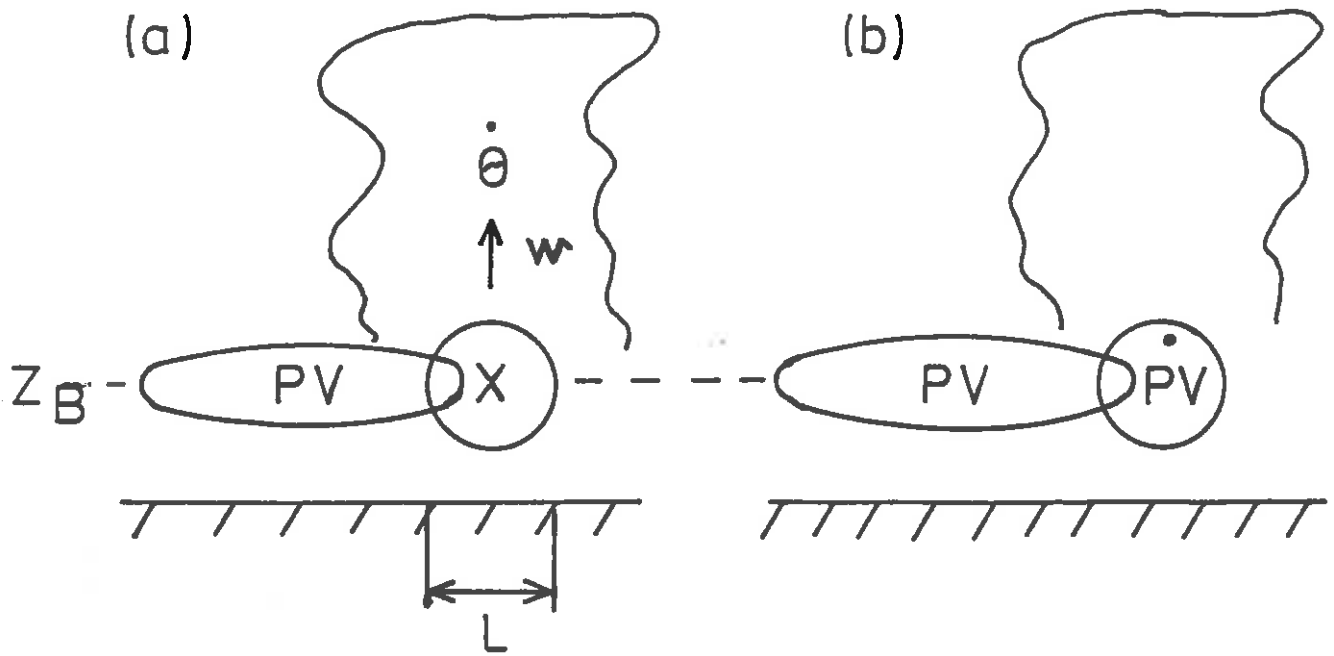


Figure 6

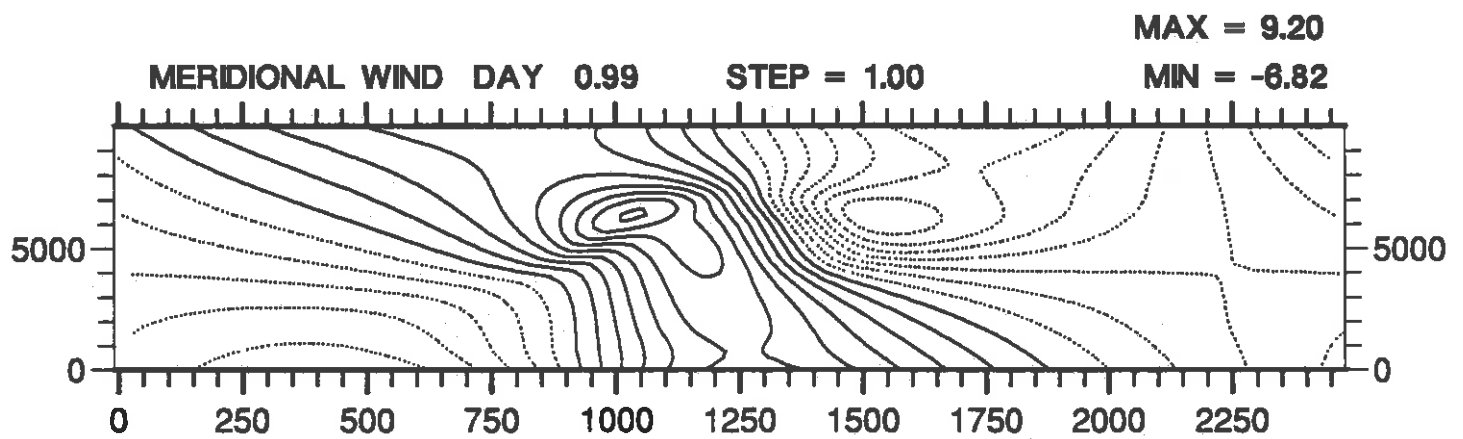
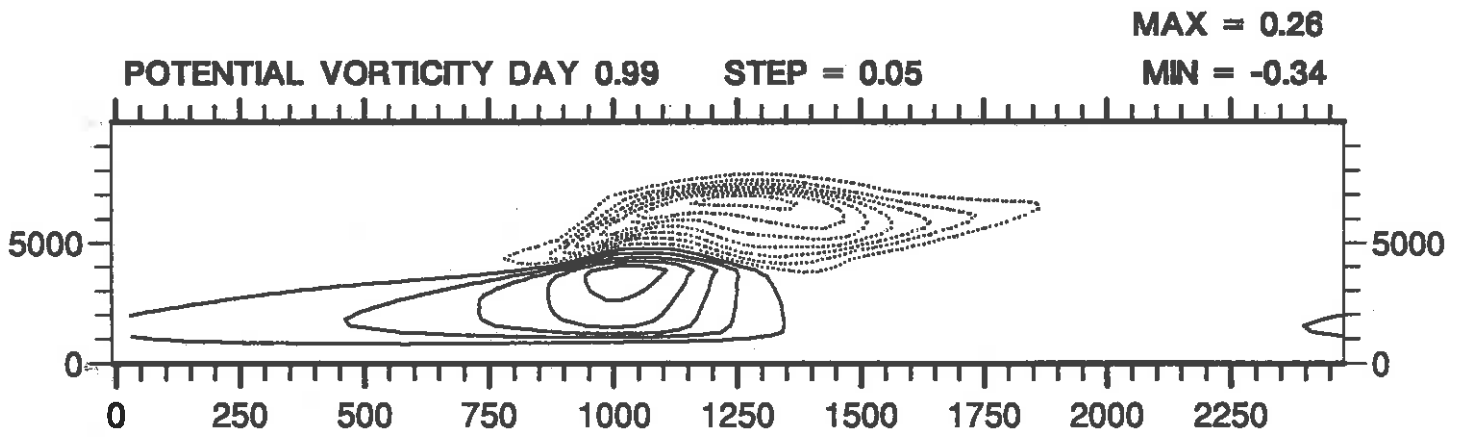


Figure 7 (1/2)

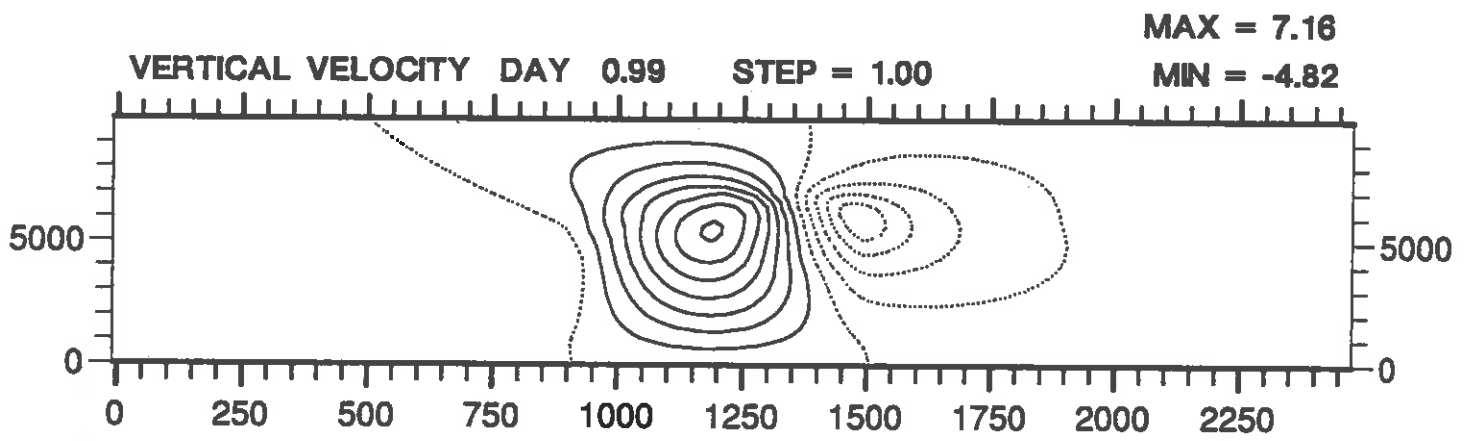


Figure 7 (2/2)

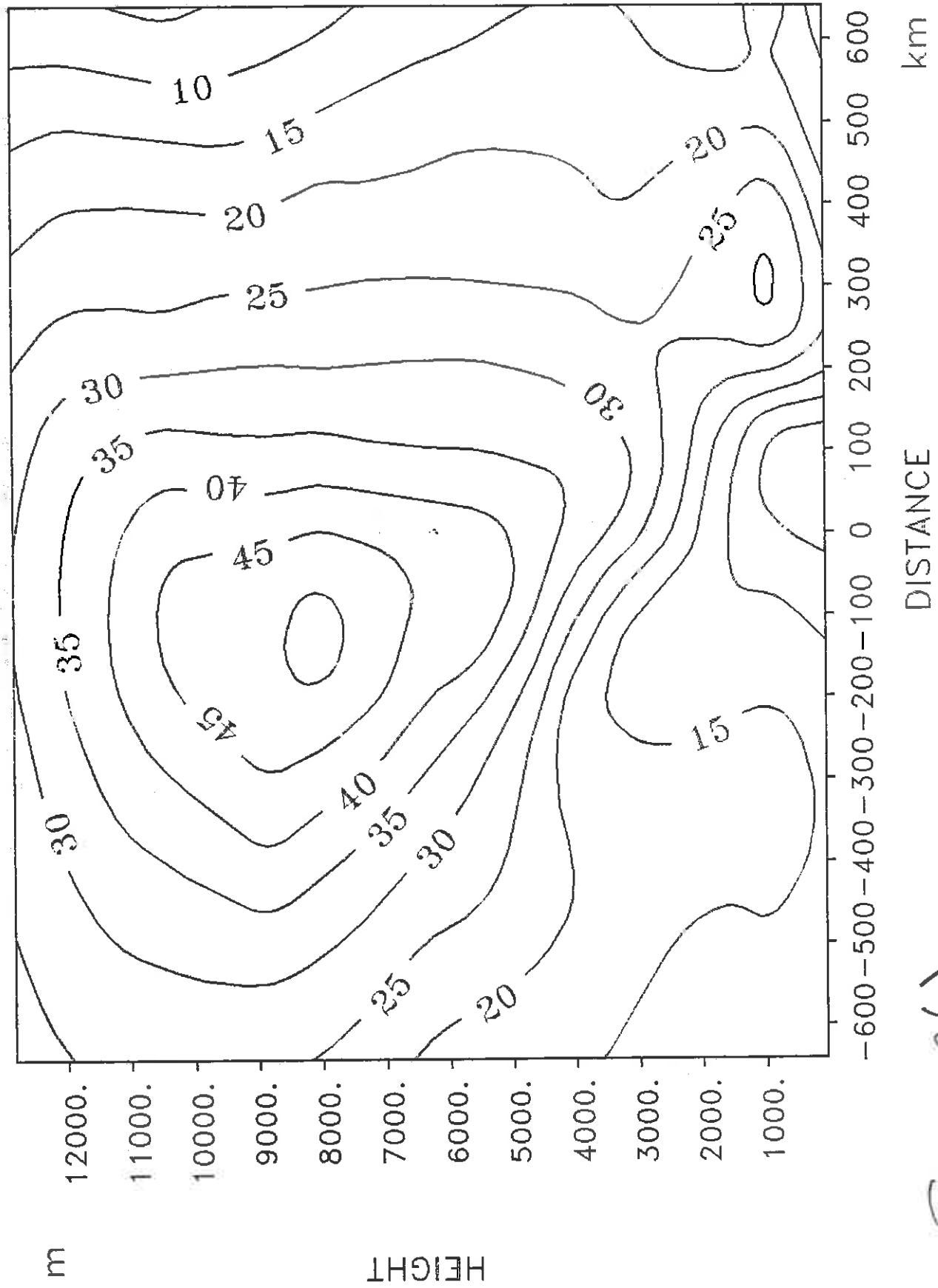


Figure 8(a)

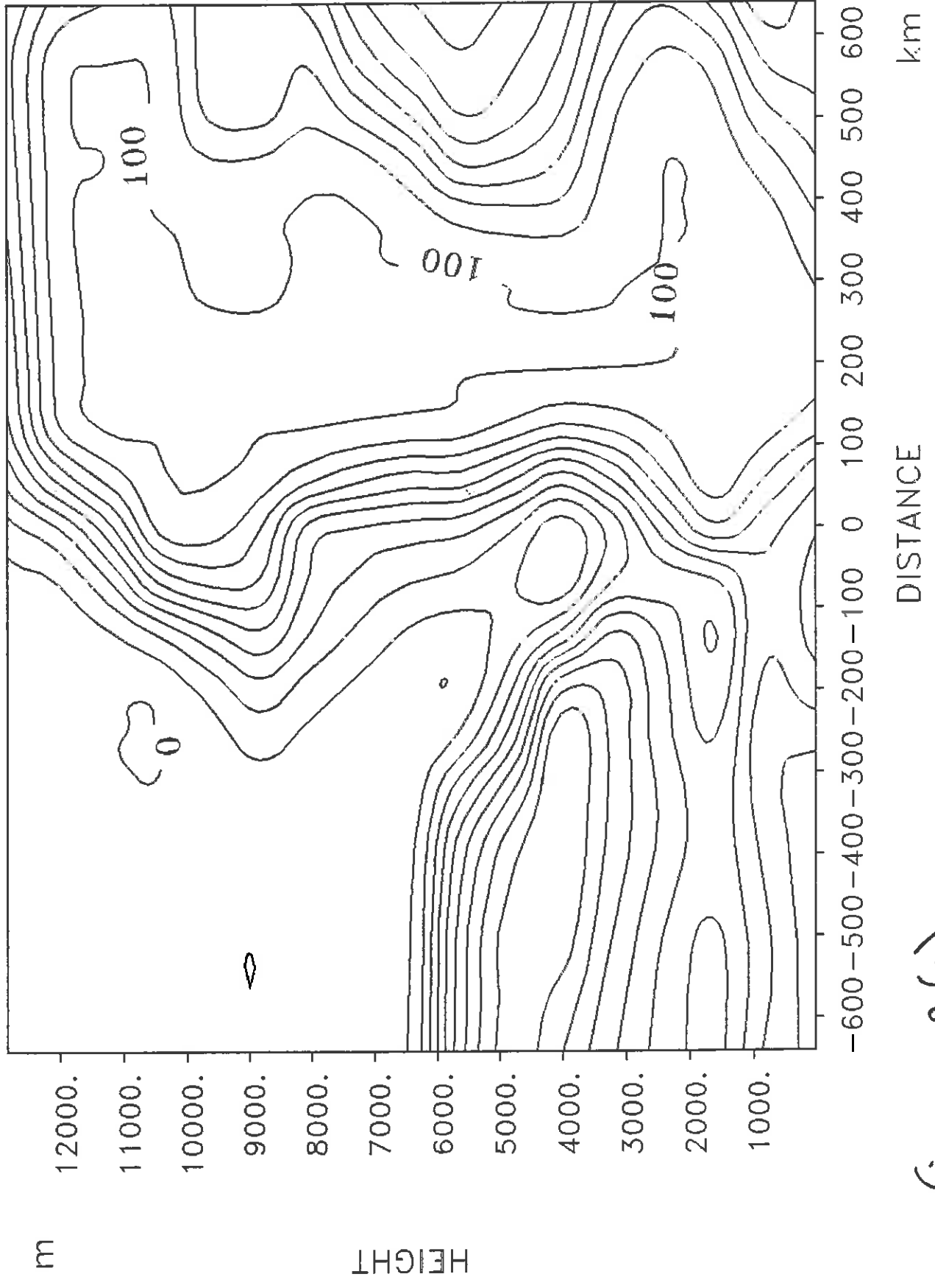


figure 8 (b)

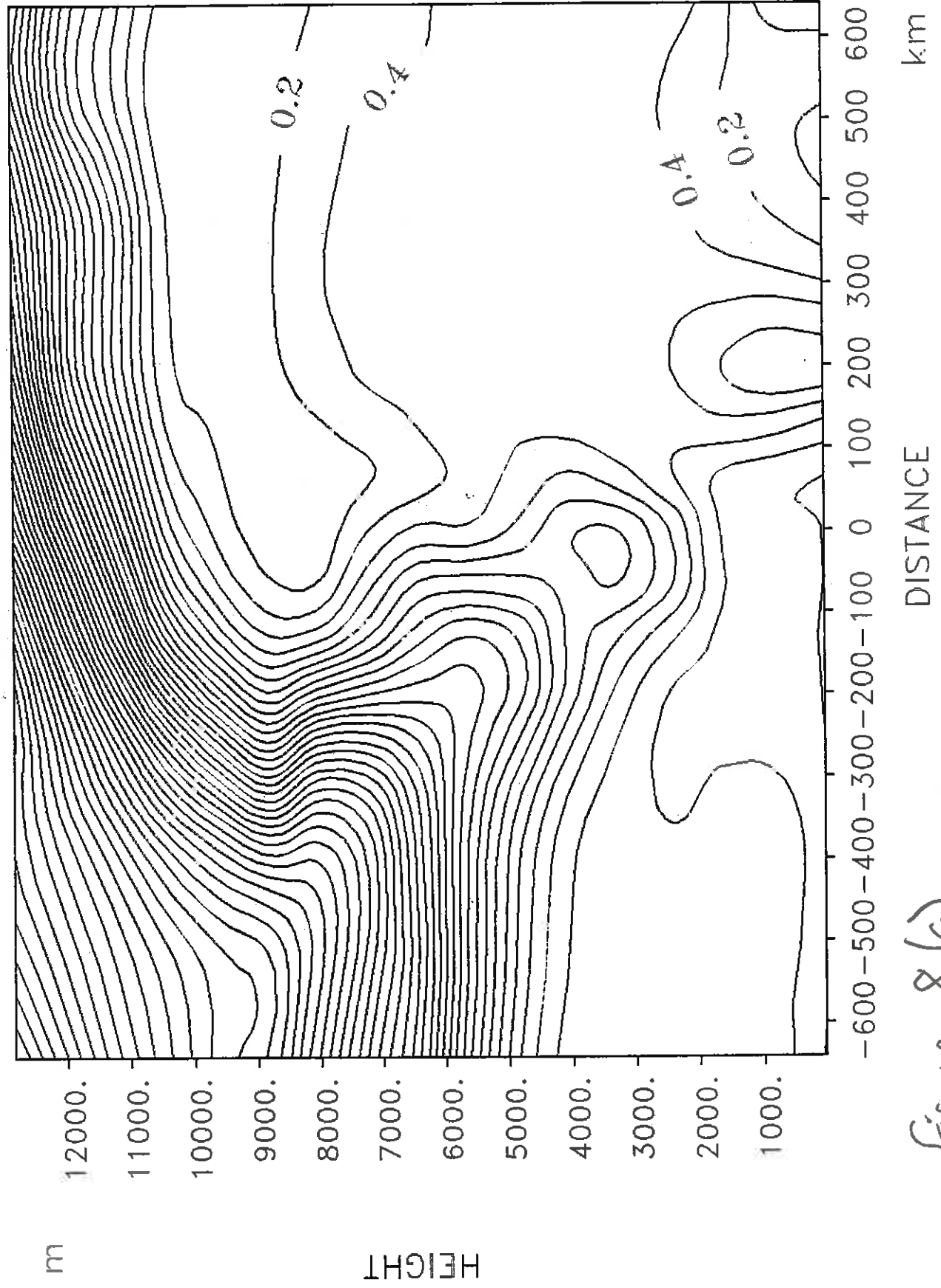


Figure 8 (c)

CURRENT JCMM INTERNAL REPORTS

This series of JCMM Internal Reports, initiated in 1993, contains unpublished reports and also versions of articles submitted for publication. The complete set of Internal Reports is available from the National Meteorology Library on loan, if required.

1. **Research Strategy and Programme.**
K A Browning et al
January 1993
2. **The GEWEX Cloud System Study (GCSS).**
GEWEX Cloud System Science Team
January 1993
3. **Evolution of a mesoscale upper tropospheric vorticity maximum and comma cloud from a cloud-free two-dimensional potential vorticity anomaly.**
K A Browning
January 1993
4. **The Global Energy and Water Cycle**
K A Browning
July 1993
5. **Structure of a midlatitude cyclone before occlusion.**
K A Browning and N Roberts
July 1993
6. **Developments in Systems and Tools for Weather Forecasting.**
K A Browning and G Szejwach
July 1993
7. **Diagnostic study of a narrow cold frontal rainband and severe winds associated with a stratospheric intrusion.**
K A Browning and R Reynolds
August 1993
8. **Survey of perceived priority issues in the parametrizations of cloud-related processes in GCMs.**
K A Browning
September 1993
9. **The Effect of Rain on Longwave Radiation.**
I Dharssi
September 1993
10. **Cloud Microphysical Processes - A Description of the Parametrization used in the Large Eddy Model.**
H Swann
October 1993

11. **An Appreciation of the Meteorological Research of Ernst Kleinschmidt.**
A J Thorpe
May 1992
12. **Potential Vorticity of Flow Along the Alps.**
A J Thorpe, H Volkert and Dietrich Heimann
August 1992
13. **The Representation of Fronts.**
A J Thorpe
January 1993
14. **A Parametrization Scheme for Symmetric Instability: Tests for an Idealised Flow.**
C S Chan and A J Thorpe
February 1993
15. **The Fronts 92 Experiment: a Quicklook Atlas.**
Edited by T D Hewson
November 1993
16. **Frontal wave stability during moist deformation frontogenesis.**
Part 1. Linear wave dynamics
C H Bishop and A J Thorpe
May 1993
17. **Frontal wave stability during moist deformation frontogenesis.**
Part 2. The suppression of non-linear wave development.
C H Bishop and A J Thorpe
May 1993
18. **Gravity waves in sheared ducts.**
S Monserrat and A J Thorpe
October 1993
19. **Potential Vorticity and the Electrostatics Analogy: Quasi-Geostrophic Theory.**
C Bishop and A J Thorpe
November 1993
20. **Recent Advances in the Measurement of Precipitation by Radar.**
A J Illingworth
April 1993
21. **Micro-Physique et Givrage. Cloud Microphysics and Aircraft Icing.**
A J Illingworth
May 1993

22. **Differential Phase Measurements of Precipitation.**
M Blackman and A J Illingworth
May 1993
23. **Estimation of Effective Radius of Cloud Particles from the Radar Reflectivity.**
N I Fox and A J Illingworth
May 1993
24. **A Simple Method of Dopplerising a Pulsed Magnetron Radar.**
L Hua, A J Illingworth and J Eastment
November 1993
25. **Radiation and Polar Lows.**
George C Craig
February 1994
26. **Collected preprints submitted to International Symposium on the Life Cycles of Extratropical Cyclones; Bergen, Norway, 27 June - 1 July 1994**
April 1994
27. **Convective Frontogenesis**
Douglas J Parker, Alan J Thorpe
April 1994

Met Office Joint Centre for Mesoscale Meteorology Department of Meteorology
University of Reading PO Box 243 Reading RG6 6BB United Kingdom
Tel: +44 (0)118 931 8425 Fax: +44 (0)118 931 8791
www.metoffice.com

